

The Electronic Structure of the Hydrogen Molecule: A Tutorial Exercise in Classical and Quantum Computation

Vincent Graves,[†] Christoph Sünderhauf,[†] Nick S. Blunt,[†] Róbert Izsák,^{*,†} and
Milán Szóri[‡]

[†]*Riverlane, St Andrews House, 59 St Andrews Street, Cambridge, CB2 3BZ, UK*

[‡]*Institute of Chemistry, University of Miskolc, Egyetemváros A/2, H-3515 Miskolc,
Hungary*

E-mail: robert.izsak@riverlane.com

Abstract

In this educational paper, we will discuss calculations on the hydrogen molecule both on classical and quantum computers. In the former case, we will discuss the calculation of molecular integrals that can then be used to calculate potential energy curves at the Hartree–Fock level and to correct them by obtaining the exact results for all states in the minimal basis. Some aspects of spin-symmetry will also be discussed. In the case of quantum computing, we will start out from the second-quantized Hamiltonian and qubit mappings. Using quantum phase estimation, we then provide the circuits for two different algorithms: Trotteization and qubitization. Finally, the significance of quantum error correction will be briefly discussed.

1 Introduction

It has been almost 20 years since Prof. Csizmadia, known simply to his students as IGC, gave a series of lectures at the University of Szeged about theoretical calculations and their relevance to organic chemistry. As students (R. I., M. Sz.) attending these lectures, we knew that he had studied with Slater and was a professor of international standing who had been associated with the University of Toronto for a long time. While we had already heard of the basics of quantum mechanics and quantum chemistry, we were all eager to know more about their applications to chemical problems that we had also encountered by then in the organic chemistry lab. Who better to tell us about that than IGC, who was among the pioneers of applying Gaussian orbitals to organic molecules and was among the authors of POLYATOM,¹⁻³ the first program package that could carry out such calculations? Despite his many scientific achievements, IGC never talked much about the past except to explain something to his students. He had a unique style that can be discerned from some of his writings⁴ but that worked best in the classroom. We all remember his simple explanations of complicated mathematical subjects, usually accompanied by student-friendly illustrations that he simply called Mickey Mouse Figures. Apart from his knowledge on chemical calculation and his accessible lecturing style, his dedication set him apart from most teachers we had known: few people would have given a two-hour long lecture when struggling with a whooping cough that threatened to strangle him. In our contribution to this special issue commemorating his achievements, we would like to pay tribute to him as an educator by providing an educational introduction to quantum chemistry methods, using the hydrogen molecule as an important first example. While IGC would have probably preferred an organic molecule and might have given less detail about the calculation than we intend to, he would have certainly approved of our using the simplest Gaussian orbital basis possible and we hope that such a simple model calculation will help the determined student to understand the machinery underlying modern quantum chemistry calculations. It is in this spirit that we offer this contribution to his memory.

2 Theoretical Background

2.1 The Hartree–Fock Method

Chemistry investigates the myriad of ways molecules may interact. With the advent of quantum mechanics, it became possible to explain these interactions in terms of those between the electrons and nuclei that make up molecules. Unfortunately, this leaves us with a large number of variables to consider if we want to describe everything that takes place in a chemist’s flask. To make the problem easier to solve, several further assumptions are made beyond the axioms of quantum mechanics and special relativity needed to describe chemical systems. To start with, akin to usual practice in thermodynamics, we may divide the universe into a system and its environment. The system is simply the part of the world we are interested in, and, for chemical purposes, this might be a number of atoms and molecules. As a first approximation, we will consider only particles in the system and neglect interactions with the environment. We will further neglect relativistic effects and the time dependence of the states of the system. Within the Born-Oppenheimer approximation, the nuclear and electronic variables are separated and the electronic problem is solved for fixed nuclear coordinates. The electronic Hamiltonian then takes the form

$$\hat{H} = - \sum_i \frac{1}{2} \nabla_i^2 + \sum_{A < B} \frac{Z_A Z_B}{|\mathbf{R}_A - \mathbf{R}_B|} - \sum_{iA} \frac{Z_A}{|\mathbf{r}_i - \mathbf{R}_A|} + \sum_{i < j} \frac{1}{|\mathbf{r}_i - \mathbf{r}_j|}, \quad (1)$$

where the indices i, j denote electrons and A, B nuclei, \mathbf{r}_i is the position of an electron and \mathbf{R}_A is that of a nucleus, Z_A is its charge number. The terms in the order they appear are the kinetic energy of the electrons, the potential energy of nuclear-nuclear, nuclear-electron and electron-electron interactions.

Although the approximations so far simplify the problem considerably, the resulting quantum mechanical problem remains intractable. In the next step, the variables describing individual electrons are also separated. To fulfil the condition of antisymmetry required by

the exclusion principle, an approximate many-electron wavefunction is constructed as the antisymmetrized product of functions describing a single electron

$$\Phi = \frac{1}{\sqrt{N!}} \begin{vmatrix} \phi_1(\mathbf{x}_1) & \phi_2(\mathbf{x}_1) & \cdots & \phi_N(\mathbf{x}_1) \\ \phi_1(\mathbf{x}_2) & \phi_2(\mathbf{x}_2) & \cdots & \phi_N(\mathbf{x}_2) \\ \vdots & \vdots & \ddots & \vdots \\ \phi_1(\mathbf{x}_N) & \phi_2(\mathbf{x}_N) & \cdots & \phi_N(\mathbf{x}_N) \end{vmatrix} \quad (2)$$

The function Φ is called the Slater determinant and the one-electron functions ϕ_p are the spin orbitals.⁴⁻⁶ Since the latter are orthonormal, the norm of Φ is also 1. The energy of the system can then be obtained as the expectation value of the Hamiltonian with respect to the Slater determinant,

$$E = \langle \Phi | \hat{H} | \Phi \rangle, \quad (3)$$

implying an integration over all electronic coordinates \mathbf{x}_p . At this point, the spin variable of an electron (s_p) can also be separated from the spatial coordinates (\mathbf{r}_p), to yield spatial orbitals φ_p ,

$$\phi_p(\mathbf{x}_p) = \varphi_p(\mathbf{r}_p)\sigma_p(s_p). \quad (4)$$

For labeling the orbitals, we will use the convention that i, j, \dots refer to orbitals occupied in the Hartree–Fock ground state, a, b, \dots are unoccupied and p, q, \dots could refer to any molecular orbital. The spin-function σ can denote a spin-up (α) or a spin-down (β) state of a single electron identified by s_p . Often, the above product is denoted simply as $p\sigma$. If necessary, spin-orbital and spatial orbital labels can be distinguished by capitalizing one of them. Here, we opt for capitalizing the spin-orbital labels, which leads to the compact notation $P = p\sigma$ or $P = p\sigma_p$. Sometimes it is convenient to refer to spin orbitals in terms of their spatial component. This purpose is served by the ‘relative’ spin notation in which the product $p\alpha$ is simply referred to as p and $p\beta$ as \bar{p} . Using the fact that the spin functions α and β are orthonormal, the following expression can be obtained for the Hartree–Fock

energy using the Slater-Condon rules⁵

$$E = \langle \Phi | \hat{H} | \Phi \rangle = E_n + 2 \sum_i (i | \hat{h} | i) + 2 \sum_{ij} (ii | jj) - \sum_{ij} (ij | ij), \quad (5)$$

where E_n is simply the nuclear-nuclear interaction term in Eq. (1). The one electron integral reads

$$(p | \hat{h} | q) = \int \varphi_p^*(\mathbf{r}) \hat{h}(\mathbf{r}) \varphi_q(\mathbf{r}) \, d\mathbf{r}, \quad (6)$$

with \hat{h} containing the kinetic energy term of the electrons and the nuclear-electron interaction energy in Eq. (1). Finally, the two-electron term is

$$(pq | rs) = \iint \frac{\varphi_p^*(\mathbf{r}_1) \varphi_q(\mathbf{r}_1) \varphi_r^*(\mathbf{r}_2) \varphi_s(\mathbf{r}_2)}{|\mathbf{r}_1 - \mathbf{r}_2|} \, d\mathbf{r}_1 d\mathbf{r}_2, \quad (7)$$

and represents the remaining electron-electron interaction term in Eq. (1). Note that these integrals are defined in terms of spatial orbitals but the spin-orbital equivalents are easily defined as $(P | \hat{h} | Q) = (p | \hat{h} | q) \delta_{\sigma_p \sigma_q}$ and $(PQ | RS) = (pq | rs) \delta_{\sigma_p \sigma_q} \delta_{\sigma_r \sigma_s}$.

To find the lowest-energy determinant Φ , the energy needs to be minimized under the constraint that Φ is normalized. This is a quite involved task in general, and in a final approximation, the molecular orbitals (MO) φ_p are expanded in terms of known atomic orbitals (AO) serving as basis functions,

$$\varphi_p = \sum_{\mu} C_{\mu p} \chi_{\mu}. \quad (8)$$

Here $C_{\mu p}$ is an element of the MO coefficient matrix \mathbf{C} . This yields the algebraic form of the Hartree-Fock equations, sometimes called the Hartree-Fock-Roothaan-Hall equations,^{4,6,7}

$$\mathbf{FC} = \mathbf{SCE}, \quad (9)$$

with the elements of the Fock matrix \mathbf{F} and the overlap matrix \mathbf{S} defined as

$$F_{\mu\nu} = \int \chi_\mu(\mathbf{r}) \hat{f}(\mathbf{r}) \chi_\nu(\mathbf{r}) \, d\mathbf{r}, \quad S_{\mu\nu} = \int \chi_\mu(\mathbf{r}) \chi_\nu(\mathbf{r}) \, d\mathbf{r}, \quad (10)$$

and \mathbf{E} being the diagonal matrix containing the molecular orbital energies. Note that from this point on we will assume that quantities are real and will not denote complex conjugation any more. As the Fock operator

$$\hat{f}[\{\varphi_i\}](\mathbf{r}_1) = \hat{h}(\mathbf{r}_1) + \sum_j \int \varphi_j(\mathbf{r}_2; \mathbf{R}) \frac{2 - \hat{P}_{12}}{|\mathbf{r}_1 - \mathbf{r}_2|} \varphi_j(\mathbf{r}_2; \mathbf{R}) \, d\mathbf{r}_2, \quad (11)$$

itself depends on the orbitals that we seek to optimize, this is a *self-consistent* eigenvalue problem, the solutions of which must be found in an iterative manner. The operator \hat{P}_{12} swaps the coordinate labels to account for antisymmetry. The resulting Fock matrix has the general form

$$F_{\mu\nu} = h_{\mu\nu} + G_{\mu\nu}, \quad (12)$$

where the core term $h_{\mu\nu}$ itself consists of two contributions,

$$h_{\mu\nu} = T_{\mu\nu} + V_{\mu\nu}, \quad (13)$$

with

$$T_{\mu\nu} = -\frac{1}{2} \int \chi_\mu(\mathbf{r}) \nabla^2 \chi_\nu(\mathbf{r}) \, d\mathbf{r}, \quad (14)$$

and

$$V_{\mu\nu} = \sum_A V_{\mu\nu}(A), \quad V_{\mu\nu}(A) = -Z_A \int \frac{\chi_\mu(\mathbf{r}) \chi_\nu(\mathbf{r})}{|\mathbf{r} - \mathbf{R}_A|} \, d\mathbf{r}, \quad (15)$$

while the electronic interaction term consists of a direct Coulomb term and an exchange term,

$$G_{\mu\nu} = \sum_{\kappa\lambda} P_{\kappa\lambda}(\mu\nu|\kappa\lambda) - \frac{1}{2} \sum_{\kappa\lambda} P_{\kappa\lambda}(\mu\kappa|\nu\lambda) \quad (16)$$

with

$$(\mu\nu|\kappa\lambda) = \iint \frac{\chi_\mu(\mathbf{r}_1)\chi_\nu(\mathbf{r}_1)\chi_\kappa(\mathbf{r}_2)\chi_\lambda(\mathbf{r}_2)}{|\mathbf{r}_1 - \mathbf{r}_2|} d\mathbf{r}_1 d\mathbf{r}_2, \quad (17)$$

where the charge-density matrix is defined as

$$P_{\kappa\lambda} = 2 \sum_i C_{\kappa i} C_{\lambda i}. \quad (18)$$

Finally, the spin-restricted Hartree–Fock (RHF) energy can be written in terms of the AO quantities as

$$E_{\text{RHF}} = E_n + \frac{1}{2} \sum_{\mu\nu} P_{\mu\nu} (h_{\mu\nu} + F_{\mu\nu}). \quad (19)$$

2.2 Electron Correlation

The Hartree–Fock solution has several deficiencies that originate in the approximations made. Over the decades several methods have been devised that improve one or more of these approximations, starting from the Hartree–Fock solution.^{6–9} Other than the choice of the AO basis, improving on the treatment of interelectronic interactions in the Hartree–Fock method is the most important issue in practical calculations. In particular, in the Hartree–Fock model, the electrons with parallel and anti-parallel spins are treated differently in that the probability of finding two electrons at the same place is zero in the former case (presence of a Fermi hole) and non-zero in the latter (lack of a Coulomb hole). This is a consequence of representing the many-body wavefunction using a single Slater determinant. However, the manifold of Slater determinants can be used to build an improved wavefunction Ψ as a linear combination

$$\Psi = \sum_I C_I \Phi_I. \quad (20)$$

If the expansion contains all possible Slater determinants in a given basis, then this full configuration interaction (FCI) expansion will yield the exact solution in that basis if the normalized coefficients C_I are optimised. To find these, the following eigenproblem must be

solved

$$\mathbf{H}\mathcal{C} = \mathcal{E}\mathcal{C}, \quad (21)$$

where \mathbf{H} is the matrix representation of the Hamiltonian with elements

$$H_{IJ} = \langle \Phi_I | \hat{H} | \Phi_J \rangle. \quad (22)$$

The correlation energy E_c is then the difference between the exact energy \mathcal{E} and the Hartree–Fock energy E ,

$$E_c = \mathcal{E} - E. \quad (23)$$

However, determinants are not the only basis in which Ψ can be expanded. Unlike determinants, configuration state functions (CSF)⁷ are eigenfunctions of the total spin squared operator,

$$\Theta = \sum_I D_I \Phi_I, \quad (24)$$

where D_I are fixed coefficients and Θ is a CSF. For a given spin sublevel, there are in fact fewer CSFs than there are determinants. Using CSFs instead of determinants may change how many basis states have large coefficients in the FCI expansion, as does rotating the orbitals between occupied and virtual spaces.

3 The Hydrogen Molecule in a Minimal Basis

3.1 Possible States and Their Long Range Behaviour

Consider a single H_2 molecule and let χ_μ be an atomic orbital⁴ (AO) on one of the H atoms, and χ_ν another AO on the other H atom. Because this simple problem has only two basis functions and is highly symmetric, it is possible to describe some of its properties, especially at large internuclear separations, even without solving the HF and FCI equations. In this section, we will discuss such general considerations, then move on to the actual calculations.

Due to the symmetries of H_2 , we know that there are only two possibilities of combining χ_μ and χ_ν into molecular orbitals. The MO coefficients must have the same magnitude with the same or opposite signs. After normalization, this yields the bonding orbital φ_i

$$\varphi_i = \frac{1}{\sqrt{2(1+S_{\mu\nu})}}(\chi_\mu + \chi_\nu), \quad (25)$$

while the anti-bonding orbital φ_a has the form

$$\varphi_a = \frac{1}{\sqrt{2(1-S_{\mu\nu})}}(\chi_\mu - \chi_\nu). \quad (26)$$

In terms of the MO coefficient matrix \mathbf{C} , this means that

$$\mathbf{C} = \begin{pmatrix} \frac{1}{\sqrt{2(1+S_{\mu\nu})}} & \frac{1}{\sqrt{2(1-S_{\mu\nu})}} \\ \frac{1}{\sqrt{2(1+S_{\mu\nu})}} & -\frac{1}{\sqrt{2(1-S_{\mu\nu})}} \end{pmatrix}. \quad (27)$$

For the purposes of analysing long range behaviour, the AOs can be assumed to be orthonormal, since the two AOs barely overlap at large bond lengths. Thus, for the remainder of this section, we will assume that $S_{\mu\nu} \approx 0$. The lowest-energy RHF determinant is then

$$\Phi_0 = |i\bar{i}|, \quad (28)$$

where

$$|i\bar{i}| \equiv |\varphi_i\bar{\varphi}_i| = \frac{1}{\sqrt{2}}(\varphi_i(1)\bar{\varphi}_i(2) - \varphi_i(2)\bar{\varphi}_i(1)). \quad (29)$$

The bar in $\bar{\varphi}_i$ denotes the fact that φ_i is occupied by a β spin orbital. Substituting Eq. (25), one gets

$$\Phi_0 = \Phi_{C0} + \Phi_{I0}, \quad (30)$$

where Φ_0 consists of a covalent part

$$\Phi_{C0} = \frac{1}{2}(|\mu\bar{\nu}| + |\nu\bar{\mu}|), \quad (31)$$

and an ionic part

$$\Phi_{I0} = \frac{1}{2}(|\mu\bar{\mu}| + |\nu\bar{\nu}|). \quad (32)$$

The covalent contribution consists of AO basis determinants in which one electron is assigned to one H atom via μ and the other electron to the other H atom via ν , which is what is expected in a homolytic dissociation process. The ionic contribution on the other hand consists of AO determinants in which both electrons are assigned to one atom only. The fact that in Φ_0 the two contributions come with an equal weight leads to what is known as the dissociation catastrophe of Hartree–Fock theory. Since Φ_{C0} describes a homolytic and Φ_{I0} a heterolytic process and since the latter requires a much higher energy, the total dissociation curve produces an artificially large dissociation energy for the homolytic process. The customary solution is to construct the doubly excited determinant

$$\Phi_1 = |a\bar{a}|, \quad (33)$$

which, after following a similar procedure as above, is found to be

$$\Phi_1 = -\Phi_{C0} + \Phi_{I0}. \quad (34)$$

We may now define a two-determinant trial wavefunction

$$\Psi_0 = \mathcal{C}_0\Phi_0 + \mathcal{C}_1\Phi_1, \quad (35)$$

which can be written as

$$\Psi_0 = (\mathcal{C}_0 - \mathcal{C}_1)\Phi_{C0} + (\mathcal{C}_0 + \mathcal{C}_1)\Phi_{I0}. \quad (36)$$

It is clear that if $\mathcal{C}_0 = -\mathcal{C}_1$, the ionic contribution vanishes and the covalent contribution survives. This trial function has the necessary flexibility to describe the entire curve in a qualitatively correct way: close to the equilibrium $\mathcal{C}_0 \approx 1$, which agrees well with the fact that HF is a good description of the H_2 molecule at equilibrium distance. This analysis is also identical with the result obtained from a valance bond (VB) construction of the wavefunction. Similar results can be obtained for the correct heterolytic curve starting from the doubly excited determinant Φ_1 .

So far we have only considered the ground state and the doubly excited state within the minimal basis. When it comes to singly excited states, it is useful to represent them using CSFs, i.e., linear combinations of determinants that are spin-eigenstates, as mentioned above. For a singlet state, this has the form

$$\Theta_S = \frac{1}{\sqrt{2}}(|i\bar{a}| - |\bar{i}a|), \quad (37)$$

This wavefunction can also be analyzed in terms of AO basis determinants,

$$|i\bar{a}| = -\Phi_{C1} + \Phi_{I1}, \quad (38)$$

$$|a\bar{i}| = \Phi_{C1} + \Phi_{I1}, \quad (39)$$

where the ionic and covalent contributions are

$$\Phi_{C1} = \frac{1}{2}(|\mu\bar{\nu}| - |\nu\bar{\mu}|), \quad (40)$$

$$\Phi_{I1} = \frac{1}{2}(|\mu\bar{\mu}| - |\nu\bar{\nu}|). \quad (41)$$

Therefore,

$$\Theta_S = \sqrt{2}\Phi_{I1}, \quad (42)$$

which means that this is a fully ionic solution at long distance. Similarly, the three degenerate

triplet states,

$$\Phi_T^+ = |ia| = -|\mu\nu|, \quad (43)$$

$$\Theta_T = \frac{1}{\sqrt{2}}(|i\bar{a}| + |\bar{i}a|) = \sqrt{2}\Phi_{C1}, \quad (44)$$

$$\Phi_T^- = |\bar{i}\bar{a}| = -|\bar{\mu}\bar{\nu}|, \quad (45)$$

all of which have a covalent character.

3.2 The Necessary Integrals

The calculation of the electronic energy requires the construction of the integrals in Eq. (10).

The simplest model that can be evaluated without the aid of a computer assumes that the basis functions χ_μ and χ_ν are simple normalized Gaussians⁴

$$\chi_\mu = \left(\frac{2\alpha}{\pi}\right)^{\frac{3}{4}} e^{-\alpha(\mathbf{r}+\mathbf{R})^2}, \quad \chi_\nu = \left(\frac{2\alpha}{\pi}\right)^{\frac{3}{4}} e^{-\alpha(\mathbf{r}-\mathbf{R})^2}, \quad (46)$$

where we have assumed that the two atoms are at an equal distance \mathbf{R} from the origin.

Without loss of generality, we may choose the molecule to lie along the x-axis, i.e., that

$\mathbf{R} = (R, 0, 0)$. Thus, the above Gaussians decompose into

$$\left(\frac{2\alpha}{\pi}\right)^{\frac{3}{4}} e^{-\alpha(\mathbf{r}\pm\mathbf{R})^2} = \left(\frac{2\alpha}{\pi}\right)^{\frac{3}{4}} e^{-\alpha(x\pm R)^2} e^{-\alpha y^2} e^{-\alpha z^2}. \quad (47)$$

While the multiplication of the same Gaussians is easily evaluated, when different Gaussians are multiplied, the Gaussian product theorem applies

$$e^{-\alpha(\mathbf{r}\pm\mathbf{R})^2} e^{-\alpha(\mathbf{r}\mp\mathbf{R})^2} = e^{-2\alpha R^2} e^{-2\alpha\mathbf{r}^2}. \quad (48)$$

The overlap integrals are then

$$S_{\mu\mu} = S_{\nu\nu} = \left(\frac{2\alpha}{\pi}\right)^{\frac{3}{2}} \int e^{-2\alpha(\mathbf{r}\pm\mathbf{R})^2} d\mathbf{r} = 1, \quad (49)$$

by normalization, and

$$S_{\mu\nu} = S_{\nu\mu} = \left(\frac{2\alpha}{\pi}\right)^{\frac{3}{2}} e^{-2\alpha R^2} \int e^{-2\alpha\mathbf{r}^2} d\mathbf{r} = e^{-2\alpha R^2}. \quad (50)$$

The two unique values of the kinetic energy integral $T_{\mu\nu}$ can be determined by using derivation and partial integration techniques. The remaining integrals contain the Coulomb operator in some form. The nuclear-electronic attraction term also depends on the position of the nuclei, yielding integrals of the form $V_{\mu\nu}(A)$ and $V_{\mu\nu}(B)$, where A and B denote the nuclei on which χ_μ and χ_ν are centered, respectively. There are altogether three unique values of these integrals, while the two-electron integrals $(\mu\nu|\kappa\lambda)$ may assume four distinct values, all listed in the Supplementary Material. We note that the evaluation of the Coulomb integrals is significantly simplified by the application of the Gaussian integral, e.g.,

$$\frac{1}{|\mathbf{r} \pm \mathbf{R}|} = \frac{1}{\sqrt{\pi}} \int_{-\infty}^{+\infty} e^{-(\mathbf{r}\pm\mathbf{R})^2 t^2} dt, \quad (51)$$

as discussed in detail elsewhere.⁷ This introduces another Gaussian function beyond the AOs χ_μ and χ_ν , and thus the usual product rules and integration techniques apply. In particular, the change of variables of the type $u^2 = t^2/(2\alpha + t^2)$ simplifies the evaluation of the integrals significantly.

Once the two-electron integrals are known, the most general form of the effective two-body term for two atomic orbitals can be written as

$$G_{\mu\mu}(\mathbf{P}) = \frac{1}{2}(\mu\mu|\mu\mu)P_{\mu\mu} + (\mu\mu|\mu\nu)P_{\mu\nu} + (\mu\mu|\nu\nu)P_{\nu\nu} - \frac{1}{2}(\mu\nu|\mu\nu)P_{\mu\nu}, \quad (52)$$

$$G_{\nu\nu}(\mathbf{P}) = (\nu\nu|\mu\mu)P_{\mu\mu} + (\nu\nu|\mu\nu)P_{\mu\nu} + \frac{1}{2}(\nu\nu|\nu\nu)P_{\nu\nu} - \frac{1}{2}(\nu\mu|\nu\mu)P_{\mu\mu}, \quad (53)$$

$$G_{\mu\nu}(\mathbf{P}) = G_{\nu\mu}(\mathbf{P}) = \frac{1}{2}(\mu\nu|\mu\mu)P_{\mu\mu} + \frac{3}{2}(\mu\nu|\mu\nu)P_{\mu\nu} + \frac{1}{2}(\mu\nu|\nu\nu)P_{\nu\nu} - \frac{1}{2}(\mu\mu|\nu\mu)P_{\mu\nu}. \quad (54)$$

Here, we have only used the fact $P_{\mu\nu}$ is symmetric.

3.3 The Orbital Exponent

These formulae can be evaluated for any R once the exponent α is known. We may determine this by assuming that the single Gaussian considered here is an STO-1G orbital, i.e., one in which a single Gaussian (1G) is used to fit a Slater type orbital (STO). The coefficient α may be obtained by maximizing the overlap⁶

$$\langle \psi_{1s} | \chi_\mu \rangle = \sqrt{\frac{\zeta_0^3}{\pi}} \left(\frac{2\alpha_0}{\pi} \right)^{\frac{3}{4}} \int e^{-\zeta_0|\mathbf{r}|} e^{-\alpha_0\mathbf{r}^2} d\mathbf{r}. \quad (55)$$

Assuming that $\zeta_0 = 1$, as in the H atom, this yields $\alpha_0 \approx 0.270950$. As α_0 is associated with $|\mathbf{r}|^2$ and ζ_0 with $|\mathbf{r}|$, it is customary⁶ to rescale α using

$$\alpha = \alpha_0\zeta^2, \quad (56)$$

if the value of ζ is different from $\zeta_0 = 1$. A change in the value of ζ would reflect the change in the STO as a result of the molecular environment. Thus, to find an optimal ζ , the energy of an H atom may be optimized as a function of ζ . This energy is simply given as

$$E_{\text{H}} = T_{\mu\mu} + V_{\mu\mu}(A) = \frac{3}{2}\alpha - 2\sqrt{\frac{2\alpha}{\pi}}, \quad (57)$$

and the optimization yields

$$\zeta = \frac{2}{3}\sqrt{\frac{2}{\pi\alpha_0}}, \quad (58)$$

yielding

$$\alpha = \frac{8}{9\pi}, \quad (59)$$

which is approximately $\alpha \approx 0.282942$. This choice of α yields the best energy value obtainable for the H atom using a single atom-centered Gaussian, $E_{\text{H}} = -4/3\pi \approx -0.424413$, still relatively far off from the exact value of $-1/2$ in atomic units.

3.4 The RHF Potential Energy Curves

The energy expression in Eq. (5) is particularly simple for the ground state of H_2 ,

$$E_0 = \langle \Phi_0 | \hat{H} | \Phi_0 \rangle = E_n + 2(i|\hat{h}|i) + (ii|ii). \quad (60)$$

Once the integrals are constructed and an initial guess of \mathbf{C} is found, the next step should be to build the Fock matrix and optimize $P_{\mu\nu}$ iteratively. Fortunately, the symmetry adapted orbitals in Eq. (25) and Eq. (26) turn out to be the self-consistent solutions of the Hartree–Fock equations. To see this, it is enough to show that $G_{\mu\mu} = G_{\nu\nu}$, since for a real symmetric two-by-two matrix with identical diagonal elements, the eigenvectors have the form (a, a) or $(a, -a)$ for some value a , usually fixed by normalization. With these assumptions, the charge density matrix is

$$\mathbf{P} = \frac{1}{1 + S_{\mu\nu}} \begin{pmatrix} 1 & 1 \\ 1 & 1 \end{pmatrix}. \quad (61)$$

Substituting this into Eqs. (52), (53), (54) leads to simplifications which are discussed in more detail in the Supplementary Material, the most important of which is that $G_{\mu\mu}(\mathbf{P}) = G_{\nu\nu}(\mathbf{P})$. Once these quantities are available, the Fock matrix can be built as in Eq. (12), while the energy can be obtained as in Eq. (19), using the integrals discussed in Sec. 3.2. These steps and the final analytic formulae are discussed in more detail in the Supplementary Material.

To obtain the doubly excited state Φ_1 , Eq. (22) should be evaluated. Fortunately, for H_2 in the minimal basis, a simpler route is available by simply relabeling all i to a in the energy

formula,

$$E_1 = \langle \Phi_1 | \hat{H} | \Phi_1 \rangle = E_n + 2(a|\hat{h}|a) + (aa|aa). \quad (62)$$

This amounts to constructing a new density,

$$\bar{\mathbf{P}} = \frac{1}{1 - S_{\mu\nu}} \begin{pmatrix} 1 & -1 \\ -1 & 1 \end{pmatrix}, \quad (63)$$

which then produces a modified $G(\bar{\mathbf{P}})$ matrix. The procedure from this point is very similar to the case of E_0 and is detailed in the Supplementary Material.

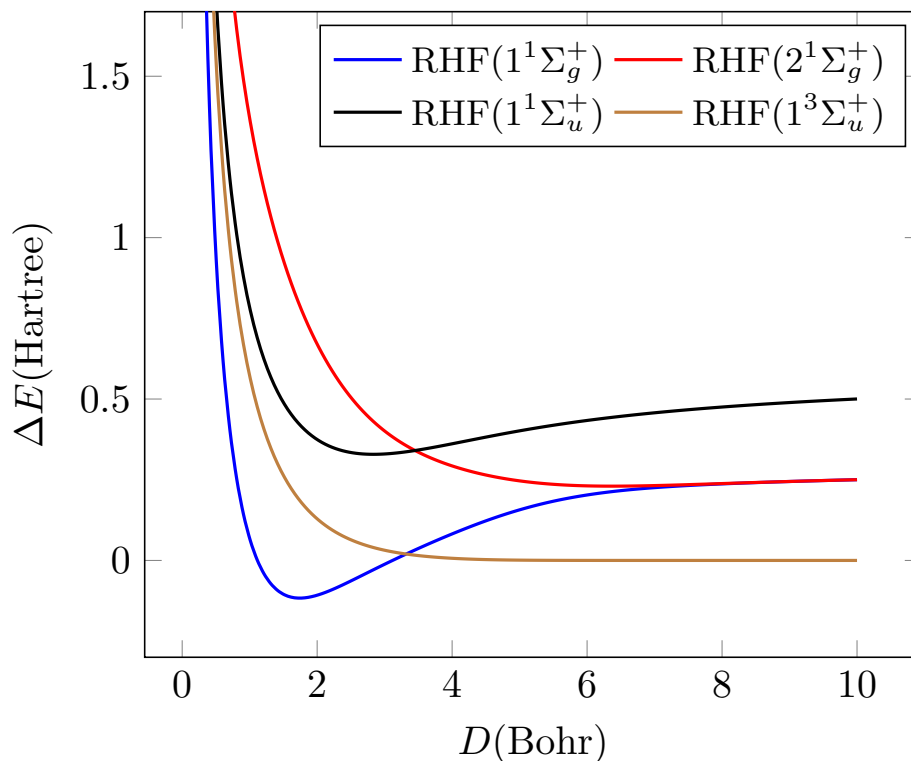


Figure 1: The RHF potential energy curves for H_2 in a minimal basis. There are three singlet and three degenerate triplet states.

Finally, the HF energies, E_S and E_T , of the singly excited singlet and triplet states can

be obtained from Eq. (22), by using the Slater-Condon rules,⁵

$$E_S = \langle \Theta_S | \hat{H} | \Theta_S \rangle = E_n + (i|\hat{h}|i) + (a|\hat{h}|a) + (ii|aa) + (ia|ia), \quad (64)$$

and

$$E_T = \langle \Theta_T | \hat{H} | \Theta_T \rangle = E_n + (i|\hat{h}|i) + (a|\hat{h}|a) + (ii|aa) - (ia|ia). \quad (65)$$

The AO expressions and the final analytical formulae are again given in the Supplementary Material.

Fig. 1 displays the dissociation curves $\Delta E_X = E_X - 2E_H$ for all the possible Hartree–Fock states in the minimal basis. Thus, E_X can be the RHF energy of the $1^1\Sigma_g^+$ singlet ground state (E_0), the doubly excited $2^1\Sigma_g^+$ singlet state (E_1), the singly excited $1^1\Sigma_u^+$ singlet state (E_S) and one of the degenerate $1^3\Sigma_u^+$ triplet states (E_T). Around the equilibrium distance, all curves behave reasonably, the ground state and the singly excited state have a minimum indicating a stable structure for H_2 in these states. As the two H atoms are pulled apart, the ground state and the doubly excited states converge. From the formulae provided in the Supplementary Material, it is easily seen that ΔE_0 and ΔE_1 both converge to the value $\sqrt{\alpha/\pi}$ as the internuclear distance D goes to infinity, while ΔE_S approaches $2\sqrt{\alpha/\pi}$ and ΔE_T goes to 0 as $D \rightarrow \infty$. The fact that the ground state curve in particular does not approach zero is often referred to as the ‘dissociation catastrophe’ of the RHF method.^{8,9} It shows that RHF does not produce two H atoms at infinite distance, but due to the weight of the ionic contributions mentioned in Sec. 3.1, it significantly overshoots, although it should be noted that it is still well under the purely ionic limit at $2\sqrt{\alpha/\pi}$. One way to solve this problem is to mix various states of the same spin and spatial symmetry; we will consider this approach in the next section.

3.5 The FCI Potential Energy Curves

To overcome the problems of the RHF method, the wavefunction can also be expanded as in Eq. (20). This means that the matrix Hamiltonian in the basis of many-electron basis states shown in Eq. (22) must be diagonalized. Notice that neither of the singlet RHF states mix with the triplet as they have different spin symmetry and Θ_S does not mix with Φ_0 or Φ_1 , as they have they have different spatial symmetry. Thus, the only non-zero off-diagonal elements in Eq. (22) are those between Φ_0 and Φ_1 , yielding a conveniently simple two-by-two matrix

$$\mathbf{H} = \begin{pmatrix} E_0 & g \\ g & E_1 \end{pmatrix}, \quad (66)$$

where $g = \langle \Phi_1 | \hat{H} | \Phi_0 \rangle = (ia|ia)$, discussed more explicitly in the Supplementary Material.

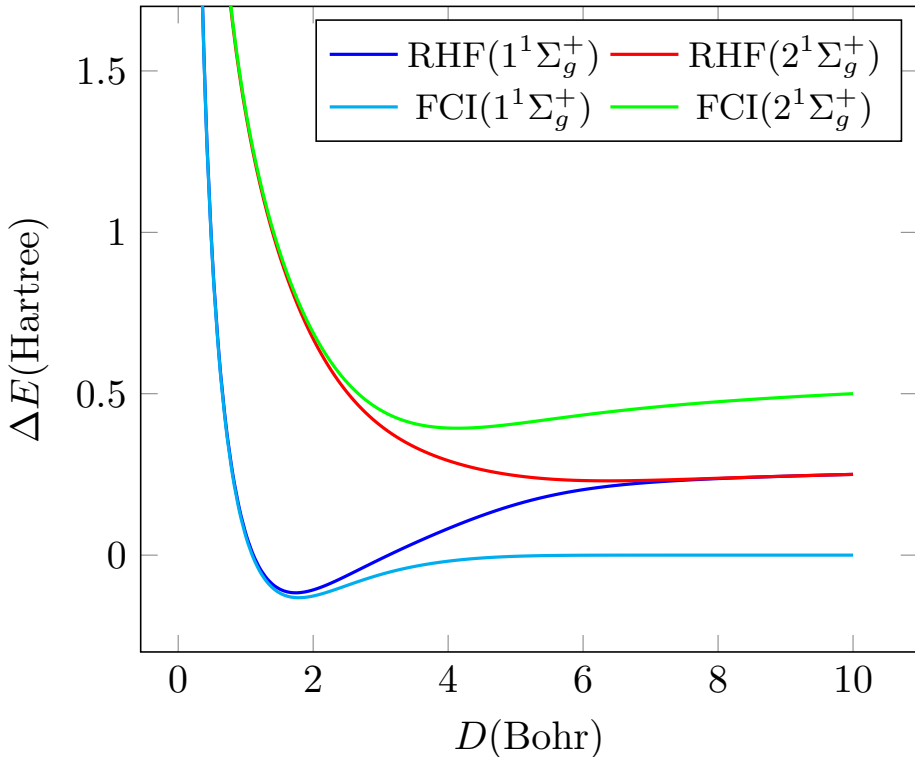


Figure 2: The FCI and the corresponding RHF potential energy curves.

As discussed before in Sec. 3.1, the mixture of Φ_0 or Φ_1 is enough to produce the correct ground-state solution in the minimal basis, due to the cancellation of ionic terms. The eigenvalues of H , shown in Fig. 2, are

$$E_{\pm} = A \pm \frac{\sqrt{\omega^2 + 4g^2}}{2}, \quad A = \frac{1}{2}(E_0 + E_1), \quad \omega = E_1 - E_0, \quad (67)$$

where A is the average RHF energy of the two states, while ω is the excitation energy. Using the formulae of the Supplementary Material, it is now easy to show that the FCI solution with the minus sign, E_- approaches 0 as $D \rightarrow \infty$ corresponding to the correct covalent dissociation limit. Furthermore, the other solution, E_+ , converges to the correct ionic limit $2\sqrt{\alpha/\pi}$. Thus, within the minimal basis, only the triplet and the singly excited singlet states are described correctly at the RHF level, it is necessary to mix two RHF states to recover the exact solutions for the other two. As we will see in the next section, there is an alternative: breaking the spin symmetry also removes the dissociation catastrophe.

3.6 The UHF Potential Energy Curves

The RHF solution in Eq. (27) has the property that $C_{\mu i} = C_{\nu i}$ and for the occupied MO i . The unrestricted Hartree–Fock (UHF) model differs from RHF in that there are two different sets of spatial orbitals for electrons with alpha and beta spins, i_{α} and i_{β} . Since these MOs span the same space as the RHF solution, we may represent them using the RHF orbitals as a basis,⁶

$$\varphi_{i_{\alpha}} = U_{ii}^{\alpha} \varphi_i + U_{ia}^{\alpha} \varphi_a, \quad (68)$$

$$\varphi_{i_{\beta}} = U_{ii}^{\beta} \varphi_i + U_{ia}^{\beta} \varphi_a. \quad (69)$$

with U^{α} and U^{β} being the unitary transformations that yield i_{α} and i_{β} . In this case, the MO coefficients belonging to the two AOs are not fixed by symmetry and need not have the same magnitude, i.e., $C_{\mu i_{\sigma}} \neq C_{\nu i_{\sigma}}$, for $\sigma = \alpha, \beta$. On the other hand, the number of alpha

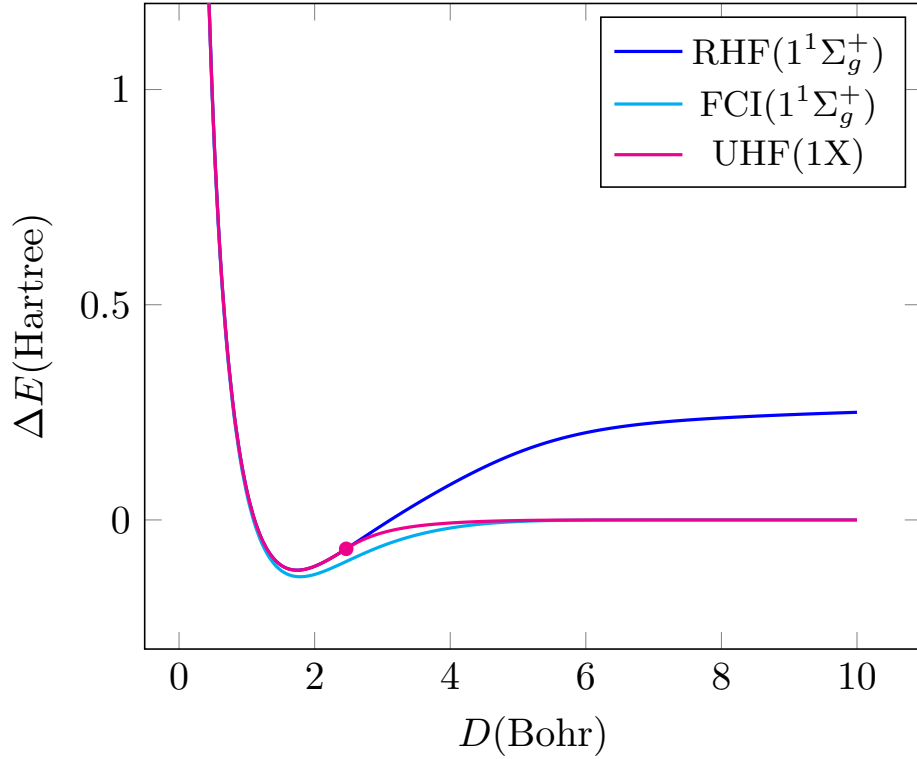


Figure 3: The RHF, UHF and FCI ground-state potential energy curves. The Coulson-Fischer point is indicated by a circle on the UHF curve.

and beta electrons are equal which is reflected in the solution: both alpha and beta orbitals can be obtained from the RHF ones by a rotation of the same angle but opposite direction, i.e., $U^\alpha = U^{\beta\dagger}$, $U_{ii}^\alpha = U_{ii}^\beta \equiv U_{ii}$ and $U_{ia}^\alpha = -U_{ia}^\beta \equiv U_{ia}$. On substitution into the UHF determinant

$$\Phi_{\text{UHF}} = |i_\alpha \bar{i}_\beta| = U_{ii}^2 \Phi_0 - U_{ia}^2 \Phi_1 + \sqrt{2} U_{ii} U_{ia} \Theta_T, \quad (70)$$

which reveals the spin-symmetry-broken nature of the UHF wavefunction since it mixes singlet and triplet states. Evaluating the energy as an expectation value gives

$$E_{\text{UHF}} = U_{ii}^4 (E_0 + E_1 + 2g - 2E_T) + 2U_{ii}^2 (E_T - E_1 - g) + E_1, \quad (71)$$

where the normalization condition was used to eliminate U_{ia} . This expression can be minimized as a function of U_{ii} with the result

$$U_{ii}^2 = \frac{E_1 + g - E_T}{E_0 + E_1 + 2g - 2E_T}. \quad (72)$$

Note that because of normalization, it must be true that $U_{ii}^2 \leq 1$. It turns out that the above function decreases monotonically as a function of D and it approached 0.5 at infinity. Thus, we need only find out where it takes the value $U_{ii} = 1$, which is the case if

$$E_0 + g - E_T = 0. \quad (73)$$

This happens at the Coulson-Fischer point at a distance of $D_{CF} = 2.4653$. Thus, the optimized UHF energy for the ground state becomes

$$E_{\text{UHF}} = \begin{cases} E_0, & D < D_{CF}, \\ E_1 - \frac{(E_1 + g - E_T)^2}{E_0 + E_1 + 2g - 2E_T}, & D_{CF} \leq D. \end{cases} \quad (74)$$

Fig. 3 shows the RHF, UHF and FCI ground-state solutions. Unlike the RHF solution, the UHF curve indeed approaches the FCI limit at infinite distance. The UHF solution is often a convenient starting point for electron correlation methods since it is a much more flexible reference point than the spin-restricted alternative, which can often only achieve a qualitatively correct starting point by mixing several determinants or CSFs. While the spin-symmetry-broken character of UHF can also be problematic,^{6,8,9} the FCI solution in Eq. (20) is much harder to obtain. Consequently, many approximate approaches have been developed on classical computers to tackle this problem, and more recently the potential benefit of quantum computers in solving this problem has also been investigated. In the next section, we will continue the discussion of the H_2 molecule from the perspective of quantum computers. In doing so, we will provide an introduction to the topic of quantum

algorithms for solving quantum chemistry problems, which is currently an active and growing area of research.

4 The Hydrogen Molecule on the Quantum Computer

4.1 The Second-Quantized Hamiltonian

Second quantization is a technique in which the evaluation of matrix elements is performed through algebraic operations. To achieve this one switches from the Hilbert-space representation to a Fock-space representation. Within the Fock space, these Slater determinants are represented as occupation number vectors (ONV), i.e., the list of the occupation numbers of orbitals in their canonical order. Next, fermionic creation and annihilation operators are defined that map ONVs onto other ONVs. If $n_P = 0, 1$ is the occupation number of spin-orbital P , which may be labelled using integers $P = 0, 1, 2, \dots$, then the annihilation and creation operators are defined by their action as

$$\hat{a}_P^\dagger |n_0, \dots, n_P, \dots, n_N\rangle = \delta_{0n_P} \Gamma_P |n_0, \dots, 1_P, \dots, n_N\rangle, \quad (75)$$

$$\hat{a}_P |n_0, \dots, n_P, \dots, n_N\rangle = \delta_{1n_P} \Gamma_P |n_0, \dots, 0_P, \dots, n_N\rangle, \quad (76)$$

where $\Gamma_P = \prod_{Q=0}^{Q=P-1} (-1)^{n_Q}$ is just a sign factor. These operators obey the following anti-commutation relations,

$$\{\hat{a}_P, \hat{a}_Q\} = 0, \quad (77)$$

$$\{\hat{a}_P^\dagger, \hat{a}_Q^\dagger\} = 0, \quad (78)$$

$$\{\hat{a}_P^\dagger, \hat{a}_Q\} = \delta_{PQ}, \quad (79)$$

and it is worth pointing out that $\delta_{PQ} = \delta_{pq} \delta_{\sigma_p \sigma_q}$, see discussion on Eq. (4). Then, the Hamiltonian can be written in terms of creation and annihilation operators, which is its

second-quantized form,

$$\hat{H} = E_n + \sum_{PQ} (P|\hat{h}|Q) \hat{a}_P^\dagger \hat{a}_Q + \frac{1}{2} \sum_{PQRS} (PS|RQ) \hat{a}_P^\dagger \hat{a}_Q^\dagger \hat{a}_R \hat{a}_S, \quad (80)$$

where the connection with the MO integrals defined previously is $(P|\hat{h}|Q) = (p|\hat{h}|q) \delta_{\sigma_p \sigma_q}$ and $(PS|RQ) = (ps|rq) \delta_{\sigma_p \sigma_s} \delta_{\sigma_r \sigma_q}$.

We next again consider the H₂ example in particular. Using the minimal basis, each of the 2 electrons can be in 4 possible states, the canonical order of which is $\varphi_i \alpha, \varphi_i \beta, \varphi_a \alpha, \varphi_a \beta$. Relabelling these as $P = 0, 1, 2, 3$, a possible two-electron state has the form $|n_0, n_1, n_2, n_3\rangle$ (with the sum of occupation numbers, i.e., the number of electrons, being 2). Due to the Pauli exclusion principle, each occupation number can be equal to 0 or 1. Thus, the lowest-energy determinant is simply $|1100\rangle$, and other determinants can be written similarly. Setting up the FCI problem would correspond to evaluating matrix elements of \hat{H} with respect to these Slater determinants. As one example, calculating $\langle 1100|\hat{H}|1100\rangle$ would yield the result in Eq. (60). We can also write the full H₂ Hamiltonian in second-quantized form. In the H₂ case, it is obvious that some of the one- and two-body integrals vanish due to spin-integration. Other terms are zero due to spatial symmetry. After simplifications, the H₂ Hamiltonian takes the form¹⁰

$$\begin{aligned} \hat{H} = E_n &+ (i|\hat{h}|i) \left(a_0^\dagger a_0 + a_1^\dagger a_1 \right) + (a|\hat{h}|a) \left(a_2^\dagger a_2 + a_3^\dagger a_3 \right) \\ &+ (ii|ii) a_0^\dagger a_1^\dagger a_1 a_0 + \overline{(ii|aa)} \left(a_0^\dagger a_2^\dagger a_2 a_0 + a_1^\dagger a_3^\dagger a_3 a_1 \right) \\ &+ (ii|aa) \left(a_0^\dagger a_3^\dagger a_3 a_0 + a_1^\dagger a_2^\dagger a_2 a_1 \right) + (aa|aa) a_2^\dagger a_3^\dagger a_3 a_2 \\ &+ (ia|ia) \left(a_0^\dagger a_3^\dagger a_1 a_2 + a_2^\dagger a_1^\dagger a_3 a_0 + a_0^\dagger a_1^\dagger a_3 a_2 + a_2^\dagger a_3^\dagger a_1 a_0 \right), \end{aligned} \quad (81)$$

where the antisymetrized integral is defined as $\overline{(ii|aa)} = (ii|aa) - (ia|ia)$. All of these integrals are known from the classical calculations in the previous section.

4.2 Second-Quantized Qubit Mappings

The basic operations on a quantum computer are carried out on two-state quantum systems called qubits. A general qubit state is an arbitrary linear combination of the $|0\rangle$ and $|1\rangle$ states, i.e. $|\psi\rangle = \alpha|0\rangle + \beta|1\rangle$, with normalization $|\alpha|^2 + |\beta|^2 = 1$.

Notice that, because each spin orbital in a chemical system can be in state $|0\rangle$ or $|1\rangle$, it seems reasonable that we can map Slater determinants, and fermionic Hamiltonians, to a qubit representation. However, the operators that act on qubits are written in terms of Pauli matrices (defined in Supplementary Material), which follow a different algebra compared to the fermionic creation and annihilation operators. Therefore, we need a way to convert the fermionic operators in the second-quantized Hamiltonian to the Pauli representation. The oldest and simplest mapping is due to Jordan and Wigner,^{10,11}

$$a_P^\dagger \rightarrow \frac{1}{2} (X_P - iY_P) \bigotimes_{Q<P} Z_Q, \quad (82)$$

$$a_P \rightarrow \frac{1}{2} (X_P + iY_P) \bigotimes_{Q<P} Z_Q, \quad (83)$$

where the sub-index indicates the qubit the matrix is acting on. Here, the string of Z operators is needed to enforce the fermionic anti-commutation relations defined in Eqs. (77) to (79).

Applying this mapping to Eq. (80) leads to the qubit Hamiltonian H , the explicit form of which can be found in the Supplementary Material for Hamiltonians with real coefficients. While the qubit Hamiltonian is quite lengthy in the general case, it assumes a relatively

simple form in the H_2 case,¹⁰

$$\begin{aligned}
H &= H_0 + H_{ii} [Z_0 + Z_1] + H_{aa} [Z_2 + Z_3] \\
&+ \frac{1}{4}(ii|ii)Z_0Z_1 + \frac{1}{4}\overline{(ii|aa)} [Z_0Z_2 + Z_1Z_3] \\
&+ \frac{1}{4}(ii|aa) [Z_0Z_3 + Z_1Z_2] + \frac{1}{4}(aa|aa)Z_2Z_3 \\
&- \frac{1}{4}(ia|ia) [X_0X_1Y_2Y_3 + Y_0Y_1X_2X_3 - X_0Y_1Y_2X_3 - Y_0X_1X_2Y_3], \tag{84}
\end{aligned}$$

with coefficients

$$H_0 = E_n + (i|\hat{h}|i) + (a|\hat{h}|a) + \frac{1}{4}(ii|ii) + \frac{1}{2}\overline{(ii|aa)} + \frac{1}{4}(aa|aa), \tag{85}$$

$$H_{ii} = \frac{1}{2}(i|\hat{h}|i) + \frac{1}{4} \left[(ii|ii) + \overline{(ii|aa)} \right], \tag{86}$$

$$H_{aa} = \frac{1}{2}(a|\hat{h}|a) + \frac{1}{4} \left[\overline{(ii|aa)} + (aa|aa) \right]. \tag{87}$$

Here, the spin-summed integral is $\overline{(ii|aa)} = 2(ii|aa) - (ia|ia)$.

There have been several alternative proposals to improve on the Jordan-Wigner mapping, both in terms of the number of qubits used and in terms of the length of the Pauli strings. A simple improvement to reduce the number of qubits required is the Qubit Efficient Encoding (QEE).¹² In this case, the mapping focuses on the fermionic ladder operators $\hat{a}_P^\dagger \hat{a}_Q$ which corresponds to sums of diadic products of basis vectors of the type $|\mathbf{n}\rangle\langle\mathbf{n}'|$, where \mathbf{n} and \mathbf{n}' are sequences of occupation numbers that differ at positions P and Q ($n_P = n'_Q = 1$, $n_Q = n'_P = 0$). To proceed further, the basis vectors are converted into a binary form based on their ordering. In the general case, the number of qubits required is only logarithmic in the number of spin orbitals. In the H_2 case, there are six possible two-electron basis states of the type $|\mathbf{n}\rangle = |n_0, n_1, n_2, n_3\rangle$ such that the occupation numbers add up to 2. In the occupation number representation, encoding $|\mathbf{n}\rangle$ requires 4 qubits. However, the six possible basis states may also be labeled as $0, \dots, 5$ by some convention. Since the binary

representation of the largest ordinal, 5, is 101 and this requires only three digits, all six states can also be represented as $|\mathbf{b}\rangle = |b_0, b_1, b_2\rangle$ using only 3 qubits. The fermionic ladder operators then also have the form $|\mathbf{b}\rangle\langle\mathbf{b}'|$ which can be decomposed into direct products of $|0\rangle\langle 0|$, $|0\rangle\langle 1|$, $|1\rangle\langle 0|$ and $|1\rangle\langle 1|$.

A separate issue with the Jordan-Wigner encoding is the long string of anti-symmetrizing Z operators that appears after the mapping, which leads to undesirable scaling. Bravyi and Kitaev proposed a new mapping which encoded this anti-symmetrization in a more efficient way.¹³ The number of qubits required still depends on the number of spin orbitals, N , but this time, the information that is stored on these qubits depends on the qubit index, starting from 0. If the index is even then the qubit is encoded with the orbital occupation, much like in Jordan-Wigner. If the index is odd then the anti-symmetrization of a subset of orbitals is encoded. Finally, when $\log_2(i + 1)$ is an integer (where i is the qubit index) then the anti-symmetrization of all orbitals with an index lower than or equal to the current index is encoded. All sums are performed in modulo 2. The Jordan-Wigner and Bravyi-Kitaev mapping have been compared in the literature for chemical calculations.¹⁴ Although the Bravyi-Kitaev approach certainly has its advantages, for our purposes, the Jordan-Wigner mapping is a sufficient starting point.

4.3 The 1-Qubit Hydrogen Hamiltonian

The symmetries present in the Hamiltonian can be exploited to reduce (or “taper”) the number of qubits required for a calculation. For the case of H_2 , note that only two Slater determinants, $|1100\rangle$ and $|0011\rangle$, can contribute to the ground-state wavefunction, due to particle number, spin and spatial symmetries. Since only two states can contribute, this suggests that the corresponding Hamiltonian can be represented by just a single qubit.

The general procedure to reduce the Hamiltonian is beyond the scope of this paper and is discussed elsewhere.^{15,16} Here, it is enough to note that we are looking for a transformation

of the type

$$H' = U^\dagger H U, \quad (88)$$

where U is unitary. Since H and H' are unitarily equivalent, their eigenvalues are also the same. The main requirement that should make this transformation worthwhile is that H' should commute with Pauli X matrices for at least some of the qubits. If this holds, then for the purposes of determining the ground-state energy, these qubits can be replaced by the eigenvalues of the corresponding X matrices, i.e., either $+1$ or -1 . In the H_2 case, U can be written¹⁵ as $U = U_1 U_2 U_3$, with

$$U_P = \frac{1}{\sqrt{2}}(X_P + Z_0 Z_P), \quad (89)$$

for $P = 1, 2, 3$. The transformation $\mathcal{P}' = U^\dagger \mathcal{P} U$ can now be performed for each Pauli string \mathcal{P} in the Jordan-Wigner qubit Hamiltonian in Eq. (84). The results are summarized in the Supplementary Material. As a consequence, only X or I matrices act on qubits 1, 2 and 3 in H' . For example, for $\mathcal{P} = Z_2$, $\mathcal{P}' = Z_0 X_2$; although there is a Z acting on qubit 0, only X or I Paulis act on qubits 1, 2 and 3.

Before these qubits can be tapered, the corresponding eigenvalues of X matrices should be known for the eigenstate of H' that we seek, which will be the ground state. Here, symmetry can again be exploited since, as noted above, it only allows the configurations $|1100\rangle$ and $|0011\rangle$ to contribute to the ground state, $|\Psi\rangle$. Therefore, the eigenvalues of the operators $Z_0 Z_1$ must be equal to $+1$, while the eigenvalue of $Z_0 Z_2$ and $Z_0 Z_3$, will equal -1 . Taking $Z_0 Z_1$ as an example, we may write

$$Z_0 Z_1 |\Psi\rangle = |\Psi\rangle. \quad (90)$$

Inserting $U U^\dagger = I$,

$$Z_0 Z_1 U U^\dagger |\Psi\rangle = |\Psi\rangle, \quad (91)$$

and applying U^\dagger to both sides gives

$$\left(U^\dagger Z_0 Z_1 U\right) U^\dagger |\Psi\rangle = U^\dagger |\Psi\rangle. \quad (92)$$

From the above, $U^\dagger |\Psi\rangle$ is an eigenvector of the transformed Hamiltonian H' and based on the results shown in the Supplementary Material, $U^\dagger Z_0 Z_1 U = X_1$. Therefore, the eigenstates of H' are also eigenstates of X_1 with eigenvalue $+1$, and all instances of X_1 in the Hamiltonian can be replaced by $+1$. The same argument can be worked through for X_2 and X_3 , which will be replaced by eigenvalues -1 .

Thus, the only operators remaining in the transformed Hamiltonian are Z_0 and X_0 acting on qubit 0, and qubits 1, 2 and 3 can be removed. The final single-qubit Hamiltonian has the form

$$H' = c_0 + c_1 Z_0 + c_2 X_0, \quad (93)$$

with

$$c_0 = H_0 + \frac{1}{4}[(ii|ii) + (aa|aa)] - \frac{1}{2}\overline{(i|aa)}, \quad (94)$$

$$c_1 = 2(H_{ii} - H_{aa}), \quad (95)$$

$$c_2 = (ia|ia). \quad (96)$$

4.4 Quantum Algorithms

Once the qubit Hamiltonian is available, the question still remains of how the energy calculation is to be carried out. In the current era of noisy intermediate scale quantum (NISQ) devices, the program depth measured in terms of the number of gates in the quantum circuit must be short enough so that the program can run before device errors ruin the result. This has led to a search for algorithmic solutions that satisfy this criteria, the most important of them for chemistry being the variational quantum eigensolver (VQE) algorithm.¹⁷ In VQE, the wavefunction is parametrized in a similar way as in traditional approaches of

quantum chemistry, such as coupled cluster theory and variational Monte Carlo, except that the quantum implementation should be unitary. Such an approach relies on Ansätze, i.e., the wavefunction is parametrized using a reference function (typically the HF solution) and parameterized quantum gates acting on it. This leads to a linear combination of excited determinants. VQE is a hybrid classical-quantum algorithm in which the energy evaluations happen on the quantum computer, while the optimization of the wavefunction coefficients is performed on the classical computer. Although this approach is more familiar to computational chemists, and for H_2 in the minimal basis it could even yield the exact energy, it has steep scaling with system size,¹⁸ and so we do not consider it further here.

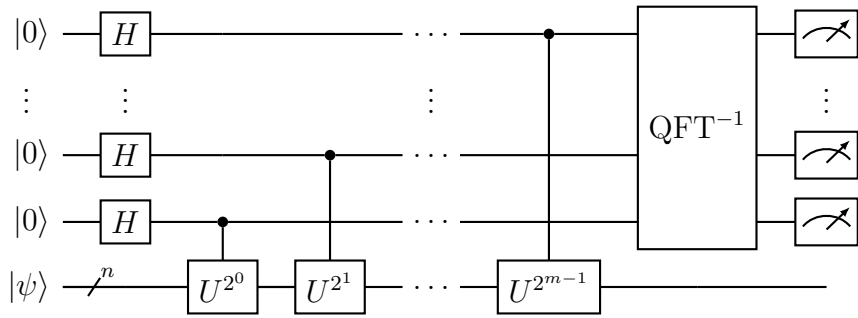


Figure 4: The “textbook” quantum phase estimation (QPE) circuit. The n data qubits are prepared in an initial state $|\psi\rangle$. The top m qubits are ancilla qubits, which are eventually measured at the end of the circuit to obtain an eigenphases of the unitary U to m bits of precision.

Quantum phase estimation (QPE), on the other hand, is a purely quantum algorithm, first introduced by Kitaev in 1995.¹⁹ The QPE method can be used to determine the eigenvalues of a unitary operator U ,

$$U|\Psi_k\rangle = e^{2\pi i\theta_k}|\Psi_k\rangle, \quad (97)$$

where θ_k is the phase corresponding to the k 'th eigenstate of U , $|\Psi_k\rangle$. The quantum circuit diagram for the “textbook” QPE algorithm²⁰ is shown in Fig. 4. The top m qubits are ancilla qubits, which are measured at the end of the circuit to obtain the first m bits of an eigenphase θ_k of U . The bottom n qubits (represented in this circuit diagram by a single line), to which the unitary U is applied, are prepared in an initial state, $|\psi\rangle$. Here, n is

the number of qubits in the Hamiltonian, which is equal to 1 for the H_2 Hamiltonian in Eq. 93. The initial state $|\psi\rangle$ should be a good approximation to the exact eigenstate $|\Psi_k\rangle$, whose eigenphase we want to estimate. The larger the overlap, the higher the probability of measuring the desired θ_k . However, in general there is a chance that the wavefunction will collapse to an undesired $|\Psi_k\rangle$ upon measurement.

Remember that our goal is to estimate the eigenvalues of H , but QPE provides the eigenphases of a unitary U . In order to apply QPE to the energy estimation problem, the eigenvalues of H must be encoded in the phases of U . Performing QPE with U will then allow estimation of the desired energies. The most common encoding of H in U is through the time evolution operator¹,

$$U(t) = e^{iHt}, \tag{98}$$

where t is a scalar parameter. If the eigenvalues of H are denoted E_k , then the eigenvalues of U will be of the form $e^{iE_k t}$, and it is trivial to obtain the desired energy from the measured eigenphase. An alternative encoding is sometimes considered in more sophisticated implementations of QPE, which is discussed in Section 4.6. To begin with, we will turn our attention to the implementation of the time evolution operator in Eq. 98. For most instances of H for chemistry problems, this cannot be implemented exactly on a quantum computer, and we instead must consider approximate approaches such as Trotterization.

4.5 Trotterization

As described in Section 4.4, we would like to perform QPE, the circuit diagram for which is shown in Fig. 4. We wish to encode the Hamiltonian in the unitary U through time evolution, as defined in Eq. 98.

For the case of H_2 in a minimal basis, the Hamiltonian consists of two single-qubit Pauli

¹Usually the time evolution operator would be e^{-iHt} , but the minus sign is unimportant in QPE, as the phases can be extracted regardless. We call $U(t)$ the time evolution operator for brevity.

operators and an identity contribution, as in Eq. 93. We drop the constant shift c_0 , so that

$$H = c_1 Z + c_2 X, \quad (99)$$

and

$$U(t) = e^{i(c_1 Z + c_2 X)t}. \quad (100)$$

Therefore we have to consider the question, how can this operator be implemented on a quantum computer? For a more general chemical Hamiltonian, its qubit form can be written

$$H = \sum_{j=1}^L H_j, \quad (101)$$

where each H_j consists of an n -qubit Pauli, P_j , and a coefficient c_j , so that $H_j = c_j P_j$, for example².

In theory, a quantum computer is capable of implementing a general unitary operation, however the number of gates required to do so may be extremely large. In practice, a finite set of basis gates is defined, from which all other unitary operations are constructed. These basis gates ultimately correspond to operations that are performed on the physical qubits. On current quantum computers, such as a superconducting quantum processor, a common set of native operations might include Pauli rotation gates, $R_P(\theta) = e^{-i(\theta/2)P}$, and a CZ (controlled Z) gate. For fault-tolerant quantum computers, arbitrary rotation gates cannot be protected, and one might instead work with the Hadamard gate, the phase gates S and T , and the CNOT gate. However, in both cases, complex multi-qubit operations such as e^{iHt} , for a general H , cannot be performed directly.

The most common solution to approximately implement $U = e^{iHt}$ for H as in Eq. 101 is through Trotter product formulas, or Trotterization. The simplest of these is the first-order

²More generally, each H_j might be a linear combination of commuting Paulis;²¹ time-evolving a Hamiltonian of fully-commuting Pauli terms can be performed efficiently. Such H_l terms are called fast-forwardable Hamiltonians.

Trotter expansion

$$e^{iHt} \approx U_1(t) = \prod_{j=1}^L e^{iH_j t}. \quad (102)$$

The second-order Trotter expansion is defined by

$$e^{iHt} \approx U_2(t) = \prod_{j=1}^L e^{iH_j t/2} \prod_{j=L}^1 e^{iH_j t/2}. \quad (103)$$

The benefit of these expansions is that each term $e^{iH_j t}$ can now be implemented in a fairly direct manner on a quantum computer. However, these product formula are approximate, unless all the terms in H commute with each other. In particular, the error on the p 'th-order Trotter expansion is²²

$$\|U_p(t) - e^{iHt}\| = \mathcal{O}(\alpha t^{p+1}). \quad (104)$$

This means that the error in the first-order expansion is $\mathcal{O}(t^2)$, while the error in the second-order expansion is $\mathcal{O}(t^3)$. The value α depends on the commutator of the terms in the partitioning of H .

In order to manage this error, we split the time evolution operator into m steps, each of length t/m :

$$e^{i\sum_l H_l t} = \left(e^{i\sum_l H_l t/m} \right)^m. \quad (105)$$

Each of the steps is then approximated by a Trotter formula, $U_p(t/m)$, which will become exact in the large- m limit.

An important question is how many rotation gates of the form $e^{iH_j t/m}$ are needed to perform time evolution up to time t with error ϵ (in the trace distance), which we denote $N_{\text{gates}}(t, \epsilon)$. This question has been studied in detail. For the first-order Trotter formula the number of required gates is²³ $N_{\text{gates}, 1}(t, \epsilon) = \mathcal{O}(t^2/\epsilon)$ while for the second-order formula²⁴ $N_{\text{gates}, 2}(t, \epsilon) = \mathcal{O}(t^{1.5}/\sqrt{\epsilon})$. For a comparison of $N_{\text{gates}}(t, \epsilon)$ for different simulation methods, see Ref. 25.

Having discussed Trotterization for general Hamiltonians, we now consider the specific

case of H_2 , taking the first-order Trotter expansion. Here we approximate $U(t)$ by

$$U(t) \approx \left(e^{iZc_1t/m} e^{iXc_2t/m} \right)^m, \quad (106)$$

so that each term is a Pauli rotation gate. In particular, the Pauli-Z rotation is defined $R_Z(\theta) = e^{-iZ\theta/2}$, and the Pauli-X rotation is $R_X(\theta) = e^{-iX\theta/2}$. Thus we have

$$U(t) \approx \left[R_Z\left(\frac{-2c_1t}{m}\right) R_X\left(\frac{-2c_2t}{m}\right) \right]^m. \quad (107)$$

Lastly, note from Fig. 4 that the U operators must each be controlled on an ancilla qubit. The circuit diagram for the controlled- U operation is shown in Figure 5.

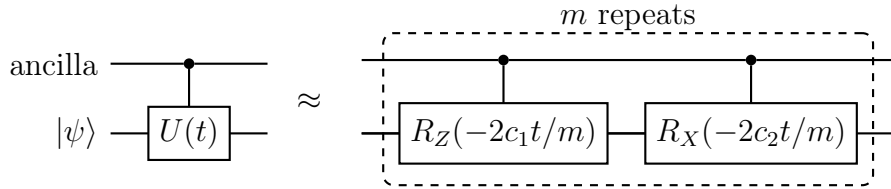


Figure 5: First-order Trotter approximation to the controlled time evolution operator, for H_2 in a minimal basis. The Trotter expansion is repeated for m steps, with the approximation becoming more accurate with larger m .

4.6 Qubitisation

Quantum phase estimation allows to measure the eigenvalues of a unitary operator U . Above, this was used to determine energies by choosing $U = e^{iHt}$ and implementing the exponential in a quantum circuit using the Trotter product formula.

Alternatively, a different unitary operator U can be chosen for phase estimation. In qubitisation,^{26,27} U is chosen to be the walk operator

$$U = e^{i \arccos(H/\lambda)}, \quad \lambda = |c_1| + |c_2| \quad (108)$$

with the subnormalisation λ the norm of the Hamiltonian³. Performing phase estimation on the walk operator also allows to determine H 's energies. Here we will specifically consider the H_2 Hamiltonian, and the constant shift c_0 will again be ignored throughout.

The walk operator can be constructed from circuits called PREPARE and SELECT using an additional ancilla qubit. The ancilla qubit's state indicates the two terms $c_1 Z$ and $c_2 X$ of the Hamiltonian. (For larger Hamiltonians with more terms, you would require more than one ancilla qubit.) The PREPARE operator acts on the ancilla qubit and *prepares* a state corresponding to the terms' coefficients c_1 and c_2 :

$$\text{PREPARE } |0\rangle = \sqrt{\frac{|c_1|}{\lambda}} |0\rangle + \sqrt{\frac{|c_2|}{\lambda}} |1\rangle = R_Y(\alpha) |0\rangle, \quad \alpha = 2 \arctan \sqrt{\left| \frac{c_2}{c_1} \right|}. \quad (109)$$

The coefficients are such that the measurement probabilities are c_1 and c_2 (here, they have the same sign, otherwise slight adaptations are necessary below), with the subnormalisation λ being required to ensure the right-hand state is normalised. PREPARE is implemented with a single-qubit rotation gate $R_Y(\alpha)$. The SELECT operator acts on the system qubit and *selects* the operator for the term corresponding to the state of the ancilla qubit. It applies either Z or X on the system qubit:

$$\text{SELECT } |0\rangle |\psi\rangle = |0\rangle Z |\psi\rangle, \quad \text{SELECT } |1\rangle |\psi\rangle = |1\rangle X |\psi\rangle. \quad (110)$$

Qubitisation theory shows that the circuit for the walk operator can be constructed from these operators together with a reflection around $|0\rangle\langle 0|$ as follows:

$$\text{ancilla } \begin{array}{|c|} \hline \text{U} \\ \hline \end{array} \begin{array}{|c|} \hline |\psi\rangle \\ \hline \end{array} = \frac{\text{PREPARE} \text{ SELECT } \text{PREPARE}^\dagger \text{ Z}}{\text{PREPARE} \text{ SELECT} \text{ PREPARE}^\dagger \text{ Z}} \quad (111)$$

For usage in the QPE circuit, the walk operator must be controlled on the ancillas that allow the readout of the phase. Inserting the circuits for PREPARE and SELECT in our example,

³To be precise, the walk operator also has eigenvalues $e^{-i \arccos(E_k/\lambda)}$.

Since a rotation by angle β_{rot} has eigenvalues $e^{\pm i\beta_{\text{rot}}}$, the walk operator has the eigenvalues $e^{\pm i \arccos(E_k/\lambda)}$ for each energy E_k of the Hamiltonian.

4.7 Quantum Error Correction

Quantum computers are affected by noise. For example, the latest IBM quantum computer³⁰ has a median error rate of $\sim 0.66\%$ for CNOT gates (noise varies strongly for different gates and gate types, but this will suffice for the following back-of-the-envelope estimation). Roughly, this means that a quantum algorithm run on such a NISQ device could only use circuits with a depth of about 103 operations before the error rate becomes larger than 50%. However, 103 gates is far too little for any useful quantum algorithm. While the error rates of qubits are expected to decrease as technology progresses, they will always stay significant compared to error rates in classical computing. This is because qubits are inherently small quantum systems and even a tiny perturbation from the environment can have a disastrous effect on the qubit's state.

Luckily, quantum error correction provides a pathway to run useful longer circuits, despite the errors affecting the qubits. To explain the concept of error correction, let us resort to the common experience of a noisy telephone line. When spelling out a name, the letters b and p can easily be confused. The error can be corrected by referring to each letter by a longer name according to the standard phonetic alphabet, like bravo for b, papa for p. This reduces the possibility of error, while increasing the length of the information transmitted. Similarly, in quantum error correction, multiple physical qubits are used to represent one logical qubit, which has a reduced error rate compared to the physical qubit.

In quantum computing, once you measure a qubit, the wavefunction collapses and the state is destroyed. This makes it difficult to correct errors that occur in the midst of a computation. However, a theory of quantum error correction has been developed and shows intricate methods to perform measurements that reveal information about errors (if any) that have occurred, without destroying the information that is encoded. This is information

is sufficient to correct the errors, provided there are not too many. For quantum algorithms of any reasonable length, we will have to resort to quantum error correction.¹⁸ While this results in an overhead in the number of physical qubits (many physical qubits encode one logical qubit) and run-time, at least it offers a chance to escape the limited fidelity of quantum computers.

5 Summary

In this contribution to the memory of Prof. Csizmadia, we have provided a detailed discussion of quantum chemical calculations on the simplest diatomic molecule, H_2 . Such a simple exercise is not only useful as an elucidation of the traditional methods of quantum chemistry, but it also serves as an introduction to the emerging field of quantum computing, as applied to chemistry. Thus, after providing a high-level overview of the theoretical basis of molecular calculations which led us to the Hartree–Fock model and to the notion of electron correlation, we turned to the evaluation of the necessary equations in the minimal basis. After a general discussion of the long-distance properties of the possible states in the minimal basis, the necessary integral calculations were outlined and the orbital exponent was determined by standard methods. Next, we have compared the spin-restricted Hartree–Fock and the exact solutions to discover that the exact solution removes the artifacts of the Hartree–Fock model and finds the proper covalent ground state. As a final contribution to our description of traditional methods, we have also discussed the effects of breaking spin-symmetry in the Hartree–Fock model. Next, we turned our attention to quantum computing and gave a brief discussion on second quantization in order to rewrite the Hamiltonian in terms of fermionic operators for the H_2 problem. We then used the Jordan-Wigner mapping to recast this Hamiltonian as a sum of Pauli-strings (products of Pauli spin-matrices) which can be implemented on a quantum computer. We have also made use of spatial symmetry to reduce the Hamiltonian to a form that acts on a single qubit. A discussion of quantum algorithms

for chemistry followed and we decided to focus on variants of quantum phase estimation in the remainder of this paper. Trotterization and qubitization were introduced as two distinct algorithms for translating the single-qubit Hamiltonian into phase estimation circuits that can in principle be run on current quantum hardware. However, in the last section on quantum error correction we also discussed why such a calculation cannot be expected to yield accurate results without applying methods to reduce noise on quantum hardware. Quantum error correction is a very active field of research and its detailed discussion is outside the scope of the present paper, although another paper is in preparation outlining its application in the case of the hydrogen molecule.³¹

References

- (1) Barnett, M. P. Mechanized Molecular Calculations—The POLYATOM System. *Rev. Mod. Phys.* **1963**, *35*, 571–572.
- (2) Csizmadia, I. G.; Harrison, M. C.; Moskowitz, J. W.; Seung, S.; Sutcliffe, B. T.; Barnett, M. P. QCPE #47.1 POLYATOM – Program set for nonempirical molecular calculations, Quantum Chemistry Exchange Program, Indiana University, Bloomington, Indiana 47401.
- (3) Csizmadia, I. G.; Harrison, M. C.; Moskowitz, J. W.; Sutcliffe, B. T. Non-empirical LCAO-MO-SCF-CI calculations on organic molecules with Gaussian type functions. *Theoretica chimica acta* **1966**, *6*, 191–216.
- (4) Csizmadia, I. G. Some Fundamentals of Molecular Orbital Computations. In *Computational Advances in Organic Chemistry: Molecular Structure and Reactivity*; Springer Netherlands: Dordrecht, 1991; pp 1–165.
- (5) Mayer, I. *Simple theorems, proofs, and derivations in quantum chemistry*; Springer Science & Business Media: New York, 2003.

- (6) Szabo, A.; Ostlund, N. S. *Modern quantum chemistry: introduction to advanced electronic structure theory*; Dover Publications: New York, 2012.
- (7) Helgaker, T.; Jorgensen, P.; Olsen, J. *Molecular electronic-structure theory*; John Wiley & Sons: New Jersey, 2014.
- (8) Bartlett, R. J.; Stanton, J. F. Applications of Post-Hartree—Fock Methods: A Tutorial. In *Reviews in Computational Chemistry*; VCH Publishers: New York, 1994; Chapter 2, pp 65–169.
- (9) Knowles, P. J.; Schütz, M.; Werner, H.-J. Ab Initio Methods for Electron Correlation in Molecules. In *Mod. Methods Algorithms Quantum Chem.*; Grotendorst, J., Ed.; NIC: Jülich, 2000; Vol. 1; pp 61–151.
- (10) Whitfield, J. D.; Biamonte, J.; Aspuru-Guzik, A. Simulation of Electronic Structure Hamiltonians Using Quantum Computers. *Mol. Phys.* **2011**, *109*, 735–750.
- (11) Jordan, P.; Wigner, E. Über das Paulische Äquivalenzverbot. *Zeitschrift für Physik* **1928**, *47*, 631–651.
- (12) Shee, Y.; Tsai, P.-K.; Hong, C.-L.; Cheng, H.-C.; Goan, H.-S. Qubit-efficient encoding scheme for quantum simulations of electronic structure. *Phys. Rev. Research* **2022**, *4*, 023154.
- (13) Bravyi, S. B.; Kitaev, A. Y. Fermionic Quantum Computation. *Annals of Physics* **2002**, *298*, 210–226.
- (14) Tranter, A.; Love, P. J.; Mintert, F.; Coveney, P. V. A comparison of the Bravyi-Kitaev and Jordan-Wigner transformations for the quantum simulation of quantum chemistry. *J. Chem. Theory Comput.* **2018**, *14*, 5617–5630.
- (15) Bravyi, S.; Gambetta, J. M.; Mezzacapo, A.; Temme, K. Tapering off qubits to simulate fermionic Hamiltonians. <http://arxiv.org/abs/1701.08213>.

- (16) Setia, K.; Chen, R.; Rice, J. E.; Mezzacapo, A.; Pistoia, M.; Whitfield, J. Reducing qubit requirements for quantum simulation using molecular point group symmetries. *J. Chem. Theory Comput.* **2020**, *16*, 6091–6097.
- (17) Peruzzo, A.; McClean, J.; Shadbolt, P.; Yung, M.-H.; Zhou, X.-Q.; Love, P. J.; Aspuru-Guzik, A.; O’Brien, J. L. A variational eigenvalue solver on a quantum processor. *Nat. Commun.* **2014**, *5*, 4213.
- (18) Blunt, N. S.; Camps, J.; Crawford, O.; Izsák, R.; Leontica, S.; Mirani, A.; Moylett, A. E.; Scivier, S. A.; Sünderhauf, C.; Schopf, P.; Taylor, J. M.; Holzmann, N. Perspective on the Current State-of-the-Art of Quantum Computing for Drug Discovery Applications. *J. Chem. Theory Comput.* **2023**, *18*, 7001–7023.
- (19) Kitaev, A. Y. Quantum measurements and the Abelian Stabilizer Problem. *arXiv:quant-ph/9511026* **1995**,
- (20) Nielsen, M. A.; Chuang, I. L. *Quantum computation and quantum information*, 10th ed.; Cambridge University Press, 2010.
- (21) Martínez-Martínez, L. A.; Yen, T.-C.; Izmaylov, A. F. Assessment of various Hamiltonian partitionings for the electronic structure problem on a quantum computer using the Trotter approximation. *arXiv:2210.10189 [quant-ph]* **2022**,
- (22) Childs, A. M.; Su, Y.; Tran, M. C.; Wiebe, N.; Zhu, S. Theory of Trotter Error with Commutator Scaling. *Phys. Rev. X* **2021**, *11*, 011020.
- (23) Lloyd, S. Universal Quantum Simulators. *Science* **1996**, *273*, 1073–1078.
- (24) Berry, D. W.; Ahokas, G.; Cleve, R.; Sanders, B. C. Efficient Quantum Algorithms for Simulating Sparse Hamiltonians. *Commun. Math. Phys.* **2006**, *270*, 359.
- (25) Childs, A. M.; Maslov, D.; Nam, Y.; Ross, N. J.; Su, Y. Toward the first quantum simulation with quantum speedup. *PNAS* **2018**, *115*, 9456.

- (26) Poulin, D.; Kitaev, A.; Steiger, D. S.; Hastings, M. B.; Troyer, M. Quantum Algorithm for Spectral Measurement with Lower Gate Count. *Phys. Rev. Lett.* **2018**, *121*, 010501.
- (27) Berry, D. W.; Kieferová, M.; Scherer, A.; Sanders, Y. R.; Low, G. H.; Wiebe, N.; Gidney, C.; Babbush, R. Improved Techniques for Preparing Eigenstates of Fermionic Hamiltonians. *npj Quantum Inf* **2018**, *4*, 22.
- (28) Ivanov, A. V.; Sünderhauf, C.; Holzmann, N.; Ellaby, T.; Kerber, R. N.; Jones, G.; Camps, J. Quantum Computation for Periodic Solids in Second Quantization. *Phys. Rev. Res.* **2023**, *5*, 013200.
- (29) Lee, J.; Berry, D. W.; Gidney, C.; Huggins, W. J.; McClean, J. R.; Wiebe, N.; Babbush, R. Even More Efficient Quantum Computations of Chemistry through Tensor Hypercontraction. *PRX Quantum* **2021**, *2*, 030305.
- (30) IBM Quantum's Highest Performant System, Yet. <https://research.ibm.com/blog/eagle-quantum-error-mitigation>.
- (31) Blunt, N. S.; Gehér, G. P.; Moylett, A. E. Compilation of a simple chemistry application to quantum error correction primitives. In preparation.

Appendix A Formulae for Energy Curves and Integrals

The kinetic energy of the electrons $T_{\mu\nu}$ is calculated as

$$T_{\mu\mu} = T_{\nu\nu} = -\frac{1}{2} \left(\frac{2\alpha}{\pi} \right)^{\frac{3}{2}} \int e^{-\alpha(\mathbf{r}\pm\mathbf{R})^2} \nabla^2 e^{-\alpha(\mathbf{r}\pm\mathbf{R})^2} d\mathbf{r} = \frac{3}{2}\alpha, \quad (116)$$

$$T_{\mu\nu} = T_{\nu\mu} = -\frac{1}{2} \left(\frac{2\alpha}{\pi} \right)^{\frac{3}{2}} \int e^{-\alpha(\mathbf{r}\pm\mathbf{R})^2} \nabla^2 e^{-\alpha(\mathbf{r}\mp\mathbf{R})^2} d\mathbf{r} = \left(\frac{3}{2}\alpha - 2\alpha^2 R^2 \right) e^{-2\alpha R^2}. \quad (117)$$

The nuclear-electronic attraction term also depends on the position of the nuclei. Let A be the atom on which χ_μ is centered and B the center of χ_ν . Then, the total potential has the form

$$V_{\mu\nu} = V_{\mu\nu}(A) + V_{\mu\nu}(B), \quad (118)$$

where the unique contributions are

$$V_{\mu\mu}(A) = V_{\nu\nu}(B) = - \left(\frac{2\alpha}{\pi} \right)^{\frac{3}{2}} \int \frac{e^{-2\alpha(\mathbf{r}\pm\mathbf{R})^2}}{|\mathbf{r}\pm\mathbf{R}|} d\mathbf{r} = -2\sqrt{\frac{2\alpha}{\pi}}, \quad (119)$$

$$V_{\mu\mu}(B) = V_{\nu\nu}(A) = - \left(\frac{2\alpha}{\pi} \right)^{\frac{3}{2}} \int \frac{e^{-2\alpha(\mathbf{r}\pm\mathbf{R})^2}}{|\mathbf{r}\mp\mathbf{R}|} d\mathbf{r} = -\frac{\text{erf}(2\sqrt{2\alpha}R)}{2R}, \quad (120)$$

$$V_{\mu\nu}(A) = V_{\mu\nu}(B) = - \left(\frac{2\alpha}{\pi} \right)^{\frac{3}{2}} e^{-2\alpha R^2} \int \frac{e^{-2\alpha\mathbf{r}^2}}{|\mathbf{r}\pm\mathbf{R}|} d\mathbf{r} = -\frac{\text{erf}(\sqrt{2\alpha}R)}{R} e^{-2\alpha R^2}. \quad (121)$$

The two-body terms can be dealt with similarly. Since there are only two basis functions, there are only four unique integrals,

$$(\mu\mu|\mu\mu) = (\nu\nu|\nu\nu) = \left(\frac{2\alpha}{\pi} \right)^3 \iint \frac{e^{-2\alpha(\mathbf{r}_1\pm\mathbf{R})^2} e^{-2\alpha(\mathbf{r}_2\pm\mathbf{R})^2}}{|\mathbf{r}_1 - \mathbf{r}_2|} d\mathbf{r}_1 d\mathbf{r}_2 = 2\sqrt{\frac{\alpha}{\pi}}, \quad (122)$$

$$(\mu\mu|\mu\nu) = (\nu\nu|\mu\nu) = \left(\frac{2\alpha}{\pi} \right)^3 e^{-2\alpha R^2} \iint \frac{e^{-2\alpha(\mathbf{r}_1\pm\mathbf{R})^2} e^{-2\alpha\mathbf{r}_2^2}}{|\mathbf{r}_1 - \mathbf{r}_2|} d\mathbf{r}_1 d\mathbf{r}_2 = \frac{\text{erf}(\sqrt{\alpha}R)}{R} e^{-2\alpha R^2}, \quad (123)$$

$$(\mu\mu|\nu\nu) = (\nu\nu|\mu\mu) = \left(\frac{2\alpha}{\pi} \right)^3 \iint \frac{e^{-2\alpha(\mathbf{r}_1\pm\mathbf{R})^2} e^{-2\alpha(\mathbf{r}_2\mp\mathbf{R})^2}}{|\mathbf{r}_1 - \mathbf{r}_2|} d\mathbf{r}_1 d\mathbf{r}_2 = \frac{\text{erf}(2\sqrt{\alpha}R)}{2R}, \quad (124)$$

$$(\mu\nu|\mu\nu) = (\nu\mu|\nu\mu) = \left(\frac{2\alpha}{\pi}\right)^3 e^{-4\alpha R^2} \iint \frac{e^{-2\alpha r_1^2} e^{-2\alpha r_2^2}}{|\mathbf{r}_1 - \mathbf{r}_2|} d\mathbf{r}_1 d\mathbf{r}_2 = 2\sqrt{\frac{\alpha}{\pi}} e^{-4\alpha R^2}. \quad (125)$$

Assuming the special form of Eq. (61) for the charge-density matrix, Eqs. (52), (53), (54) of the main text take the following special form,

$$G_{\mu\mu}(\mathbf{P}) = G_{\nu\nu}(\mathbf{P}) = \frac{1}{1 + S_{\mu\nu}} \left(\frac{1}{2}(\mu\mu|\mu\mu) + (\mu\mu|\mu\nu) + \frac{1}{2}(\mu\mu|\nu\nu) \right), \quad (126)$$

$$G_{\mu\nu}(\mathbf{P}) = G_{\nu\mu}(\mathbf{P}) = \frac{1}{1 + S_{\mu\nu}} ((\mu\mu|\mu\nu) + (\mu\nu|\mu\nu)), \quad (127)$$

where we have also neglected the exchange contributions in Eqs. (52), (53), (54) as they cancel some of the Coulomb terms in a system of two electrons in which the same spatial orbital is occupied by the two electrons. Putting all these results together, the Hartree-Fock energy for the hydrogen ground state can be calculated from the special case of Eq. (19),

$$E_0 = E_n + \frac{1}{1 + S_{\mu\nu}} (h_{\mu\mu} + h_{\mu\nu} + F_{\mu\mu} + F_{\mu\nu}), \quad (128)$$

leading to

$$E_0 = \frac{1}{D} + \frac{1}{1 + e^{-\frac{\alpha D^2}{2}}} \left[3\alpha - 4\sqrt{\frac{2\alpha}{\pi}} - \frac{2 \operatorname{erf}(2\sqrt{\alpha}D)}{D} + \left(3\alpha - \alpha^2 D^2 - \frac{8 \operatorname{erf}(\sqrt{\alpha}D)}{D} \right) e^{-\frac{\alpha D^2}{2}} \right. \\ \left. + \frac{1}{1 + e^{-\frac{\alpha D^2}{2}}} \left(\sqrt{\frac{\alpha}{\pi}} + \frac{4 \operatorname{erf}(\frac{\sqrt{\alpha}}{2}D)}{D} e^{-\frac{\alpha D^2}{2}} + \frac{\operatorname{erf}(\sqrt{\alpha}D)}{2D} + 2\sqrt{\frac{\alpha}{\pi}} e^{-\alpha D^2} \right) \right]. \quad (129)$$

Here a change of variables $2R = D$ was also introduced so that the expressions depend directly on the internuclear distance D .

A similar process yields the following simplified G -elements corresponding to $\bar{\mathbf{P}}$ in Eq. (63),

$$G_{\mu\mu}(\bar{\mathbf{P}}) = G_{\nu\nu}(\bar{\mathbf{P}}) = \frac{1}{1 - S_{\mu\nu}} \left(\frac{1}{2}(\mu\mu|\mu\mu) - (\mu\mu|\mu\nu) + \frac{1}{2}(\mu\mu|\nu\nu) \right), \quad (130)$$

$$G_{\mu\nu}(\bar{\mathbf{P}}) = G_{\nu\mu}(\bar{\mathbf{P}}) = \frac{1}{1 - S_{\mu\nu}} ((\mu\mu|\mu\nu) - (\mu\nu|\mu\nu)), \quad (131)$$

and a new energy expression

$$E_1 = E_{nn} + \frac{1}{1 - S_{\mu\nu}}(h_{\mu\mu} - h_{\mu\nu} + F_{\mu\mu} - F_{\mu\nu}), \quad (132)$$

and finally,

$$E_1 = \frac{1}{D} + \frac{1}{1 - e^{-\frac{\alpha D^2}{2}}} \left[3\alpha - 4\sqrt{\frac{2\alpha}{\pi}} - \frac{2 \operatorname{erf}(2\sqrt{\alpha}D)}{D} - \left(3\alpha - \alpha^2 D^2 - \frac{8 \operatorname{erf}(\sqrt{\alpha}D)}{D} \right) e^{-\frac{\alpha D^2}{2}} \right. \\ \left. + \frac{1}{1 - e^{-\frac{\alpha D^2}{2}}} \left(\sqrt{\frac{\alpha}{\pi}} - \frac{4 \operatorname{erf}(\frac{\sqrt{\alpha}}{2}D)}{D} e^{-\frac{\alpha D^2}{2}} + \frac{\operatorname{erf}(\sqrt{\alpha}D)}{2D} + 2\sqrt{\frac{\alpha}{\pi}} e^{-\alpha D^2} \right) \right]. \quad (133)$$

For the singly-excited singlet state, the AO basis expression has the form

$$E_S = \langle \Theta_S | \hat{H} | \Theta_S \rangle = E_n + (P_{\mu\mu} + \bar{P}_{\mu\mu})(\mu | \hat{h} | \mu) + (P_{\mu\nu} + \bar{P}_{\mu\nu})(\mu | \hat{h} | \nu) \\ + P_{\mu\mu} \bar{P}_{\mu\mu}(\mu\mu | \mu\mu) + P_{\mu\nu} \bar{P}_{\mu\nu}(\mu\nu | \mu\nu), \quad (134)$$

yielding

$$E_S = \frac{1}{D} + \frac{1}{1 - e^{-\frac{\alpha D^2}{2}}} \left(3\alpha - 4\sqrt{\frac{2\alpha}{\pi}} - \frac{2 \operatorname{erf}(2\sqrt{\alpha}D)}{D} \right) \\ - \frac{e^{-\frac{\alpha D^2}{2}}}{1 - e^{-\frac{\alpha D^2}{2}}} \left(3\alpha - \alpha^2 D^2 - \frac{8 \operatorname{erf}(\sqrt{\alpha}D)}{D} \right) + 2\sqrt{\frac{\alpha}{\pi}}. \quad (135)$$

Similarly for the triplets

$$E_T = \langle \Theta_S | \hat{H} | \Theta_S \rangle = E_n + (P_{\mu\mu} + \bar{P}_{\mu\mu})(\mu | \hat{h} | \mu) + (P_{\mu\nu} + \bar{P}_{\mu\nu})(\mu | \hat{h} | \nu) \\ + P_{\mu\mu} \bar{P}_{\nu\nu}(\mu\mu | \nu\nu) + P_{\mu\nu} \bar{P}_{\mu\nu}(\mu\nu | \mu\nu), \quad (136)$$

so that

$$\begin{aligned}
E_T &= \frac{1}{D} + \frac{1}{1 - e^{-\frac{\alpha D^2}{2}}} \left(3\alpha - 4\sqrt{\frac{2\alpha}{\pi}} - \frac{2 \operatorname{erf}(2\sqrt{\alpha}D)}{D} \right) \\
&\quad - \frac{e^{-\frac{\alpha D^2}{2}}}{1 - e^{-\frac{\alpha D^2}{2}}} \left(3\alpha - \alpha^2 D^2 - \frac{8 \operatorname{erf}(\sqrt{\alpha}D)}{D} \right) \\
&\quad + \frac{1}{1 - e^{-\frac{\alpha D^2}{2}}} \left(\frac{\operatorname{erf}(\sqrt{\alpha}D)}{D} - 2\sqrt{\frac{\alpha}{\pi}} e^{-\frac{\alpha D^2}{2}} \right). \tag{137}
\end{aligned}$$

Finally, the off-diagonal element in the FCI-matrix in Eq. (66) is simply given as

$$g = \langle \Phi_1 | \hat{H} | \Phi_0 \rangle = (ia|ia) = \frac{1}{1 - e^{-\alpha D^2}} \left(\sqrt{\frac{\alpha}{\pi}} - \frac{\operatorname{erf}(\sqrt{\alpha}D)}{D} \right). \tag{138}$$

Appendix B Qubit Mappings

Any 2×2 matrix can be written as a linear combination of the Pauli spin-matrices X , Y , and Z and the identity matrix I given by

$$X = \begin{pmatrix} 0 & 1 \\ 1 & 0 \end{pmatrix} \quad Y = \begin{pmatrix} 0 & -i \\ i & 0 \end{pmatrix} \quad (139)$$

$$Z = \begin{pmatrix} 1 & 0 \\ 0 & -1 \end{pmatrix} \quad I = \begin{pmatrix} 1 & 0 \\ 0 & 1 \end{pmatrix} \quad (140)$$

For a general chemical Hamiltonian with real coefficients, the explicit form of the qubit Hamiltonian in terms of MO integrals, after applying the Jordan-Wigner mapping, is

$$\begin{aligned} \mathcal{H} = & E_n + \frac{1}{2} \left[\sum_P (P|\hat{h}|P) + \frac{1}{4} \sum_{PQ} \overline{(PP|QQ)} \right] \\ & - \frac{1}{2} \sum_P \left[(P|\hat{h}|P) + \frac{1}{2} \sum_Q \overline{(PP|QQ)} \right] Z_P + \frac{1}{4} \sum_{Q<P} \overline{(PP|QQ)} Z_P Z_Q \\ & + \frac{1}{2} \sum_{Q<P} \left[(P|\hat{h}|Q) + \frac{1}{4} \sum_R \overline{(PQ|RR)} \right] (X_P \cdot X_Q + Y_P \cdot Y_Q) \\ & - \frac{1}{4} \sum_{P<Q<R} \overline{(PQ|RR)} Z_R (X_Q \cdot X_P + Y_Q \cdot Y_P) \\ & - \frac{1}{4} \sum_{P<R<Q} \overline{(PQ|RR)} (X_Q \cdot R \cdot X_P + Y_Q \cdot R \cdot Y_P) \\ & - \frac{1}{4} \sum_{R<P<Q} \overline{(PQ|RR)} (X_Q \cdot X_P + Y_Q \cdot Y_P) Z_R \\ & - \frac{1}{4} \sum_{S<R<Q<P} [(PS|QR) - (PQ|SR)] (X_P \cdot X_Q X_R \cdot X_S + Y_P \cdot Y_Q Y_R \cdot Y_S) \\ & - \frac{1}{4} \sum_{S<R<Q<P} [(PR|QS) - (PQ|RS)] (X_P \cdot X_Q Y_R \cdot Y_S + Y_P \cdot Y_Q X_R \cdot X_S) \\ & - \frac{1}{4} \sum_{S<R<Q<P} [(PS|QR) - (PR|QS)] (X_P \cdot Y_Q Y_R \cdot X_S + Y_P \cdot X_Q X_R \cdot Y_S). \end{aligned} \quad (141)$$

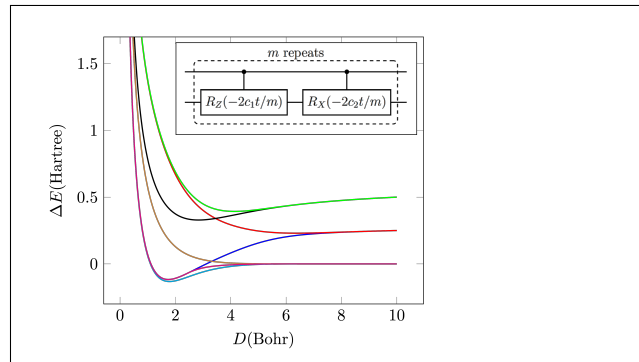
Here the notation $X_Q.X_P = X_Q Z_{Q-1} \dots Z_{P+1} X_P$ indicates a product of Z_S matrices such that $P < S < Q$, while $X_Q.R.X_P$ denotes a similar string, except that $S \neq R$.

Appendix C The 1-Qubit Hydrogen Hamiltonian

The transformed Pauli strings in the Jordan-Wigner Hamiltonian, after performing $\mathcal{P} \rightarrow \mathcal{P}' = U^\dagger \mathcal{P} U$ as defined in the main text, are as follows:

$$\begin{array}{c}
 \left[\begin{array}{c}
 Z_0 \\
 Z_1 \\
 Z_2 \\
 Z_3 \\
 Z_0 Z_1 \\
 Z_0 Z_2 \\
 Z_0 Z_3 \\
 Z_1 Z_2 \\
 Z_1 Z_3 \\
 Z_2 Z_3 \\
 Y_0 Y_1 X_2 X_3 \\
 X_0 Y_1 Y_2 X_3 \\
 Y_0 X_1 X_2 Y_3 \\
 X_0 X_1 Y_2 Y_3
 \end{array} \right] \rightarrow \left[\begin{array}{c}
 Z_0 \\
 Z_0 X_1 \\
 Z_0 X_2 \\
 Z_0 X_3 \\
 X_1 \\
 X_2 \\
 X_3 \\
 X_1 X_2 \\
 X_1 X_3 \\
 X_2 X_3 \\
 X_0 X_2 X_3 \\
 X_0 X_3 \\
 X_0 X_1 X_2 \\
 X_0 X_1
 \end{array} \right] \tag{142}
 \end{array}$$

TOC Graphic



The potential energy curves of H_2 and a simple quantum circuit associated with them.